

서브미크론 리소그래피를 위한 4 반사광학계의 설계 Four-mirror optical system for UV submicron lithography

박 성 잔, 이 상 수

한국과학기술원, 물리학과

A design of a four-mirror optical system for submicron lithography using KrF excimer laser beam($\lambda=248\text{nm}$) is presented. By using the third order aberration theory, analytic solutions for a telecentric, flat-field, and anastigmatic four-spherical-mirror system (reduction magnification $5\times$) are found. Aspherization is carried out to the spherical mirror surfaces in order to reduce the residual higher order aberrations and vignetting effect. Finally we obtain a reflection system useful in submicron lithographic application.

1. INTRODUCTION

The optical system designs for submicron lithography have advanced toward the system with larger numerical aperture(N.A.) and shorter wavelength.^{1,2} They are usually composed of numerous refractive lenses, but these systems have several inherent disadvantages such as chromatic aberrations and restriction in the choice of optical glass at shorter wavelength. Below the i-line(365 nm), especially at 248nm of the KrF excimer laser beam, only fused silica and crystal halides are available, and this makes it more difficult to correct the chromatic aberrations.

These difficulties due to the optical materials may be overcome immediately by using all reflective system that is free from chromatic aberrations. In 1975, Offner proposed the new optical system for a $1\times$ projection printer that made use of the annular field concept.³ It is a concentric two-spherical-mirror system with three reflections. All the third order aberrations of the system are eliminated. However, this system works only at unit magnification, and residual aberrations limit the useful zone width to several millimeters.

Meanwhile, four-mirror systems composed of two units of two-mirror system were reported, but most of these systems are telescopes for infrared imagery.⁴⁻⁸ It is well known that inverse Cassegrainian system is

anastigmatic and has a range of magnification.^{9,10} Also, the Petzval sum of Cassegrainian configuration may have opposite sign to that of inverse Cassegrainian configuration. These previous works indicate that it may be possible to nullify spherical aberration, coma, astigmatism, and Petzval sum of the four-spherical-mirror system composed of the Cassegrainian-inverse Cassegrainian configuration.

In this paper, we report our work to develop, by use of the third order Seidel aberration theory and optimization technique, a four-mirror lithographic projection system with reduction magnification($5\times$). Our goal is to improve the performances of the system to the extent that it should fulfill all the requirements^{11,12} of the lithographic projection optics and be expected to have diffraction limited performance at the wavelength of the KrF excimer laser with N.A. of 0.25 over an image field diameter of 10mm.

2. ANALYSES OF THE FLAT-FIELD, ANASTIGMATIC CONDITIONS OF THE FOUR-SPHERICAL-MIRROR SYSTEM

The schematic diagram of the Cassegrainian-inverse Cassegrainian system is depicted in Fig. 1. In this system, the aperture stop lies on the third mirror(c_3 in Fig. 1), and the principal ray makes angle β with the optical

axis at the stop. Magnification($M=1/m$) of the system and the third order Seidel aberration coefficients¹³ for spherical aberration(S_I), coma(S_{II}), astigmatism(S_{III}), and Petzval sum(S_{IV}) are expressed in terms of Gaussian brackets,¹⁴⁻¹⁷ as

$$S_I = -2u_o^4 (X - c_4 g_7^2 a_4^2) , \quad (1)$$

$$S_{II} = -2u_o^3 \beta (Y - c_4 g_7^2 a_4 b_4) , \quad (2)$$

$$S_{III} = -2u_o^2 \beta^2 (Z - c_4 g_7^2 b_4^2) , \quad (3)$$

$$S_{IV} = 2H^2 (c_1 - c_2 + c_3 - c_4) , \quad (4)$$

$$M = 1/m$$

$$= 1/[d_0, 2c_1, -d_1, -2c_2, d_2, 2c_3, -d_3, -2c_4] . \quad (5)$$

where X, Y, Z are defined as

$$X = c_1 g_1^2 a_1^2 - c_2 g_3^2 a_2^2 + c_3 g_5^2 a_3^2 ,$$

$$Y = c_1 g_1^2 a_1 b_1 - c_2 g_3^2 a_2 b_2 + c_3 g_5^2 a_3 b_3 ,$$

$$Z = c_1 g_1^2 b_1^2 - c_2 g_3^2 b_2^2 + c_3 g_5^2 b_3^2 ,$$

and

$$g_1 = [d_0] ,$$

$$g_3 = [d_0, 2c_1, -d_1] ,$$

$$g_5 = [d_0, 2c_1, -d_1, -2c_2, d_2] ,$$

$$g_7 = [d_0, 2c_1, -d_1, -2c_2, d_2, 2c_3, -d_3] ,$$

$$a_1 = [d_0, c_1] ,$$

$$a_2 = [d_0, 2c_1, -d_1, -c_2] ,$$

$$a_3 = [d_0, 2c_1, -d_1, -2c_2, d_2, c_3] ,$$

$$a_4 = [d_0, 2c_1, -d_1, -2c_2, d_2, 2c_3, -d_3, -c_4] ,$$

$$b_1 = [c_1, -d_1, -2c_2, d_2] ,$$

$$b_2 = [-c_2, d_2] ,$$

$$b_3 = 1 ,$$

$$b_4 = [-d_3, -c_4] .$$

In these equations, $c_i(i=1,2,3,4)$ is the curvature of each mirror, $d_i(i=0,1,2,3,4)$ is the distance between mirrors, as shown in Fig. 1, and $u_i(i=0,1,2,3,4)$ is the convergence angle of the ray from the axial object point. H is Lagrange invariant, and symbol of $[]$ denotes Gaussian bracket. It is worth mentioning here that X, Y and Z are independent of d_3 and c_4 . For the system to be flat-field and anastigmatic, four aberration coefficients given in Eqs. (1), (2), (3), and (4) should be equal to zero. From Eq. (4), the Petzval sum is zero, provided that

$$c_4 = c_1 - c_2 + c_3 . \quad (6)$$

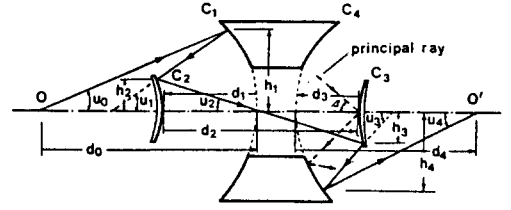


Fig. 1. Typical configuration of the four-spherical-mirror system.

Then, Equation (5) gives the expression for d_3 , which is

$$d_3 = \frac{m + 2c_4 g_5 - g_6}{2c_4 g_6} , \quad (7)$$

where $g_6 = [d_0, 2c_1, -d_1, -2c_2, d_2, 2c_3]$. Finally after some arrangement of Eqs. (1), (2), and (3) using Eqs. (6) and (7) we obtain

$$c_3 = \frac{s_4 q_1^2 + q_3 (q_2 s_1 - s_2 q_1)}{q_1 (q_3 s_1 - s_3 q_1) - q_2 (q_2 s_1 - s_2 q_1)} , \quad (8)$$

$$c_3^2 q_1 + c_3 q_2 + q_3 = 0 , \quad (9)$$

$$c_3^3 w_1 + c_3^2 w_2 + c_3 w_3 + w_4 = 0 . \quad (10)$$

In Eqs. (8), (9), and (10), note that coefficients s_i, q_i , and w_i are functions of system parameters of d_0, c_1, d_1, c_2 , and d_2 , i.e., $s_i = s_i(d_0, c_1, d_1, c_2, d_2)$, $q_i = q_i(d_0, c_1, d_1, c_2, d_2)$, and $w_i = w_i(d_0, c_1, d_1, c_2, d_2)$. Thus flat-field, anastigmatic four-spherical-mirror system with a reduction magnification should satisfy the Eqs. (6), (7), (8), (9), and (10) simultaneously. Now, note that c_4 in Eq. (6) is independent of d_3 , and the right-hand side of Eq. (8) does not contain c_3, d_3 , and c_4 . As Eqs. (9) and (10) are higher order equations of c_2 and d_2 , an elaborate procedure is required to solve these equations.

3. ANALYTIC SOLUTIONS OF THE TELECENTRIC, FLAT-FIELD, ANASTIGMATIC FOUR-SPHERICAL-MIRROR SYSTEM

We have eight-parameters for four-spherical-mirror system, but to satisfy flat-field, anastigmatic conditions with magnification($M=1/m=1/5$), we lose five-degrees of freedom. Also, by setting $c_1=-1$ for scaling of the system, there are finally only two parameters remaining,

i.e., d_0 and d_1 . The minus sign for c_1 indicates the Cassegrainian or Gregorian system for the front two-mirror system. For appropriate initial values of d_0 and d_1 , simultaneous equations given by Eqs. (9) and (10) with Eq. (8) are solved by extensive computer calculation with optimization technique.¹⁸ In this procedure, the design parameters c_2 and d_2 are decided consequently. When they are inserted into Eqs. (8), (6), and (7) sequentially, the remaining design parameters of the system c_3 , c_4 , and d_3 are determined. Thus, by repetitive application of this procedure to the proper range of d_0 and d_1 , analytic solutions of the flat-field, anastigmatic four-spherical-mirror system with reduction magnification($5\times$) are found.

The system can be realistic, however, only when they fulfill the conditions $d_2 > |d_1|$, $d_3 < 0$, $d_4 > |d_3|$, and $t = d_1 + d_2 + d_3 > 0$. An additional constraint we impose for the practical reason is that the diameter of any of the remaining mirrors should not exceed two times the diameter of the primary mirror.

Figure 2(a) illustrates the regions in which the realistic systems exist with $c_1 = -1$. There exists only Cassegrainian-inverse Cassegrainian configuration. The variation of distortion $S_5 (= S_5/2u_0\beta^3)$ as a function of d_1 for several d_0 's is shown in Fig. 2(b). Figure 2(b) reveals that the distortion free system does not exist in these four-spherical-mirror systems, hence we like to take as smaller d_0 and $|d_1|$ as possible. However, when $|d_1|$ is too small, the obscuration by the second mirror is increased and also t -value tends to be larger as shown in Fig. 2(c), which makes distance between the primary and the last mirror be long. Meanwhile, if $|d_1|$ is too large, the ratio of the diameter of last mirror(h_4) to that of primary mirror(h_1) becomes larger as shown in Fig. 2(d). So that we select the solutions with smaller

d_0 and proper $d_1 < -0.18$, which is the condition for the system with less than 50% central obscuration by second mirror.

Within the third order aberration theory, the shift of stop does not alter any aberration if the system is flat-field and anastigmatic.¹³ Therefore, by placing the aperture stop of the system at the object side focus, we can easily obtain telecentric optical system in the image space. The design data of the system selected from the Seidel solutions with good performances are listed in Table I after shifting of stop. To meet our goal, the system is scaled up to have $c_1 = -0.037522\text{cm}^{-1}$ and focal length $f' = -10\text{cm}$ with no optimization.

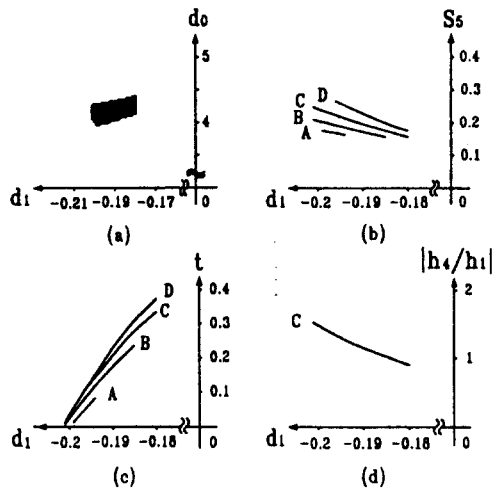


Fig. 2. Analysis of the flat-field, anastigmatic four-spherical-mirror system with $c_1 = -1$. (a) Regions where the useful systems exist, (b) Variation of $S_5 (= S_5/2u_0\beta^3)$, (c) Behavior of $t (= d_1 + d_2 + d_3)$, and (d) Behavior of $|h_4/h_1|$ as a function of d_1 for the given d_0 . (A : $d_0 = 4.0$, B : $d_0 = 4.1$, C : $d_0 = 4.2$, D : $d_0 = 4.3$).

Table I. The design data of the telecentric, flat-field, anastigmatic four-spherical-mirror system. Curvatures and distances are normalized with respect to $|c_1| = 0.037522\text{cm}^{-1}$ and $|c_1^{-1}| = 26.65103\text{cm}$, respectively.

	Mirror No.					
	Object	Stop	I	II	III	IV
Curvature			-1.000000	-0.669422	1.370190	1.039612
Distance	1.876096	2.173904	-0.195000	1.012156	-0.729388	

Figure 3 shows the residual finite ray aberrations of the system. It exhibits the expected aberration properties; i.e., the spherical aberration, coma, astigmatism, and field curvature are well corrected. And distortion in half field angle of 1° is about 0.025% which corresponds to $0.44\mu\text{m}$ over an image field diameter of 3.5mm. Figure 3(e) illustrates the tangential direction cosine of the principal ray in the image space. If it is zero over a full field, the system is completely telecentric. Because it is less than 3×10^{-5} , this system is sufficiently telecentric. For the amount of light(100%) from an axial object point reaching the image plane, the variation of the relative amount of light passing through the system is shown in Fig. 3(f) by tracing 336 finite rays from an each object field point. It is 47% for a margin field.

In summary, the telecentric, flat-field, anastigmatic four-spherical-mirror system has N.A. of 0.15 at the wavelength of KrF excimer laser, and diffraction limited performance over image field diameter of 3.5mm. The overall performances are limited mainly by distortion and vignetting, so the system at this stage may be useful

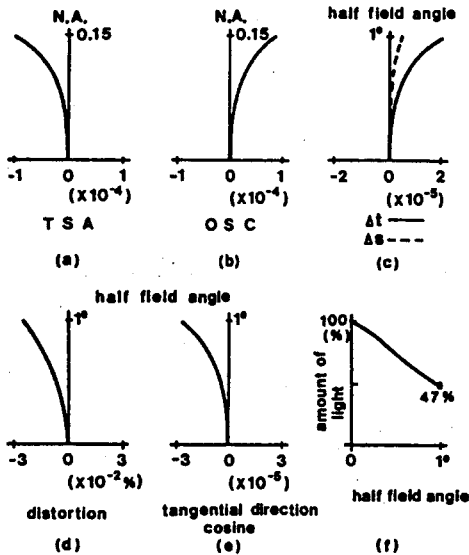


Fig. 3. (a), (b), (c), (d) are the residual finite ray aberrations of the telecentric, flat-field, anastigmatic four-spherical-mirror system, (e) tangential direction cosine of principal ray in image space, and (f) relative amount of light passing through the system. (TSA : tangential spherical aberration, OSC : offense against sine condition, Δt : tangential ray aberration, Δs : sagittal ray aberration).

in a scanning lithography¹⁹ which uses a small field of view.

4. RESIDUAL ABERRATION CORRECTION BY ASPHERIZATION

In the axially symmetric four-mirror systems, it is common that the vignetting effect becomes larger as the numerical aperture is reduced. Therefore, large extended fields are possible only in a large numerical aperture, and in the large numerical aperture system, higher order aberrations become significant. By adding aspheric terms of higher than fourth power to the mirrors, considerably high level of aberration correction is attainable. An aspheric surface used is represented by

$$z = \frac{cy^2}{1 + (1 - c^2y^2)^{1/2}} + a_4y^4 + a_6y^6 + a_8y^8 + a_{10}y^{10}, \quad (11)$$

where c is the curvature of the surface, $a_i(i=4,6,8,10)$ is coefficient of departure from the base sphere, and y is the marginal ray height at the surface.

At the first step, we have introduced departures from spherical form, on the all mirrors, depending on the fourth, sixth, eighth, and tenth powers of the aperture, as shown in Eq. (11). Next we optimize the system, by using a simple damped least squares method, with the Seidel solution obtained in Sec. 3 as a starting point. In this process, the first-order layouts of the system, i.e., magnification($M=1/5$), telecentric condition, focal length($f'=-20\text{cm}$) are fixed. These constraints are set up from the three given parameters d_{0a} , d_{a1} , and c_1 , which are the distance between object and stop, distance between stop and primary mirror, and curvature of the primary mirror, respectively. The expressions for these parameters are

$$d_{0a} = -5 f', \quad (12)$$

$$d_{a1} = f' [-d_1, -2c_2, d_2, 2c_3, -d_3, -2c_4], \quad (13)$$

$$c_1 = - \frac{1 + f' [-2c_2, d_2, 2c_3, -d_3, -2c_4]}{2f' [-d_1, -2c_2, d_2, 2c_3, -d_3, -2c_4]}. \quad (14)$$

In reducing the higher order residual aberrations, we have paid special attention on the minimization of distortion not corrected in four-spherical-mirror system. Also, vignetting effect is considered. Those systems with more than 50% central obscuration during the

optimization process are all discarded. The spot diagrams are plotted by finite ray tracing and compared with the Airy disk for the 248nm wavelength.

The data of the system found to have diffraction limited performance are listed in Table II. In an effort to reduce the distortion and vignetting, a bit strongly aspheric surfaces are used for the second and third mirrors, which are hyperboloids. The ray paths through the system for an axial pencil of light are drawn in Fig. 4, and central obscuration is less than 40%.

Figure 5 illustrates the residual finite ray aberrations of this aspherized four-mirror system. Aberrations are significantly corrected, consequently numerical aperture is increased up to 0.25, and field angle is extended to 3° , which corresponds to about 10mm in an image field diameter ($f' = -20\text{cm}$). The distortion of the system is pincushion-shaped and about 0.002%, that is, $0.1\mu\text{m}$ in a margin field, which is small enough to satisfy the requirement of the submicron lithographic optics.^{11,12} Tangential direction cosine of principal ray, as shown in Fig. 5(e), is less than 2×10^{-5} , so that the system is sufficiently telecentric. Figure 5(f) illustrates the relative amount of light (100% for the axial ray) passing through

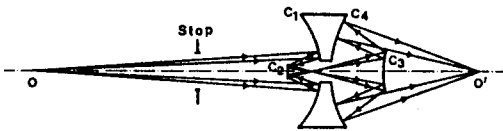


Fig. 4. Configuration of the aspherized four-mirror system.

the system over fields. It is about 90% for a margin field and 95% for a 0.7 field, which are close to the uniform illumination required in the lithographic projection optics. The number of rays traced is 404 over each field.

Meanwhile, astigmatism is slightly increased in the optimization process. However, within the half field angle

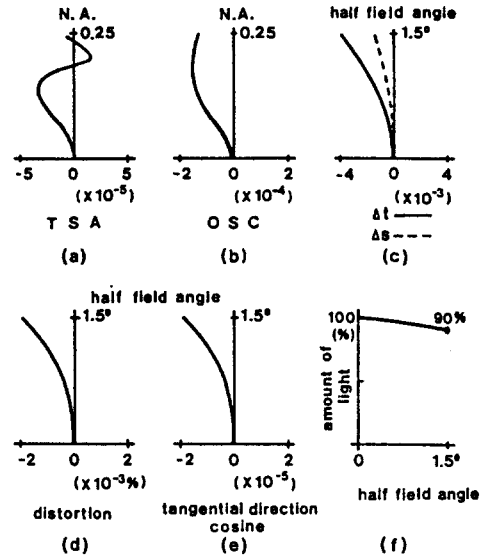


Fig. 5. (a), (b), (c), (d) are the residual finite ray aberrations of the aspherized four-mirror system, (e) tangential direction cosine of principal ray in image space, and (f) relative amount of light passing through the system. (TSA : tangential spherical aberration, OSC : offense against sine condition, Δt : tangential ray aberration, Δs : sagittal ray aberration).

Table II. The design data of the aspherized four-mirror system.

	Mirror No.					
	Object	Stop	I	II	III	IV
			ellipsoid	hyperboloid	hyperboloid	ellipsoid
Curvature(cm^{-1})			-0.019948	-0.020666	0.014452	0.015170
a_4 (cm^{-3})			0.1385×10^{-6}	0.2418×10^{-5}	-0.1329×10^{-5}	-0.1426×10^{-7}
a_6 (cm^{-5})			0.4873×10^{-9}	-0.9097×10^{-8}	0.1346×10^{-8}	0.1519×10^{-11}
a_8 (cm^{-7})			-0.2287×10^{-11}	0.1143×10^{-8}	0.1120×10^{-10}	0.7282×10^{-14}
a_{10} (cm^{-9})			0.5368×10^{-14}	-0.1593×10^{-10}	-0.9089×10^{-13}	-0.7437×10^{-17}
Distance(cm)	100.0	75.540471	-20.496044	57.895532	-32.426218	

of 1.5° and depth of focus of $2\mu\text{m}$, it has not a significant effect on the image spot, as shown in Fig. 6 and Fig. 7. Figure 6 illustrates the encircled energy calculated with the assumption that each ray carries the same amount of light energy. Figure 7 shows spot diagrams for three field angles and five defocused image positions. Figure (6) and (7) show that all of the rays fall within a circle with the radius of $0.6\mu\text{m}$ over a full field, which gives diffraction limited performance within the N.A. of 0.25, and the depth of focus of $2\mu\text{m}$ over a full field. In the same figure, circle denotes the Airy disk for KrF excimer laser beam ($\lambda=248\text{nm}$).

5. CONCLUSION

By using third order aberration theory, we have numerically obtained analytic solutions²⁰ for the telecentric, flat-field, anastigmatic four-spherical-mirror system and have found that this system has small numerical aperture and field size due to residual aberrations and vignetting. The system may be useful only in a scanning type lithography.

Through the aspherization of mirrors, however, we have improved its performances further, and the system with reduction magnification(5 \times), image field diameter of 10mm, and depth of focus of $2\mu\text{m}$ is obtained. The numerical aperture of this system is 0.25, which gives practical resolution of $0.8\mu\text{m}$ calculated from generally used criteria.^{2,11} As a whole, the four-mirror system developed in this work has reasonable performances for use as a submicron lithographic projection system.

6. REFERENCES

1. H. L. Stover, "Lens specifications and distortions," in *Optical Microlithography VI*, H. L. Stover, ed., Proc. SPIE 772, 2-4 (1987).
2. J. H. Bruning, "Lithographic lenses for microcircuit fabrication," *Opt. News* 14(6), 23-24 (1988).
3. A. Offner, "New concepts in projection mask aligners," *Opt. Eng.* 14(2), 130-132 (1975).
4. D. R. Shafer, "Four-mirror unobscured anastigmatic telescopes with all-spherical surfaces," *Appl. Opt.* 17 (7), 1072-1074 (1978).
5. J. M. Rodgers, "Nonstandard representations of aspheric surfaces in a telescope design," *Appl. Opt.* 23(4), 520-522 (1984).
6. J. M. Sasian, "Flat-field, anastigmatic, four-mirror

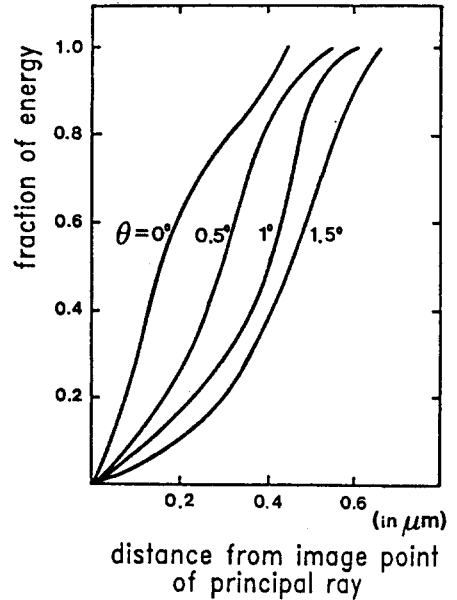


Fig. 6. Encircled energy of the aspherized four-mirror system. θ is half field angle between the axis and principal ray at the stop in Fig. 4.

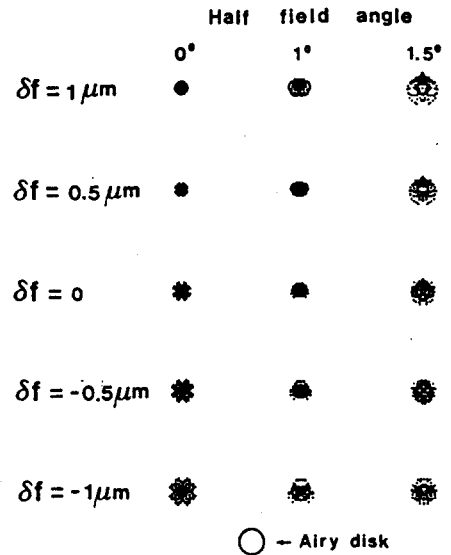


Fig. 7. Spot diagrams of the aspherized four-mirror system for three half field angles at five defocused image positions. The circle shows the size of the Airy disk for KrF excimer laser beam.

- optical system for large telescopes," *Opt. Eng.* 26 (12), 1197-1199 (1987).
7. J. U. Lee and S. S. Lee, "All-spherical four-mirror telescopes corrected for three Seidel aberrations," *Opt. Eng.* 27(6), 491-497 (1988).
 8. S. Y. Rah and S. S. Lee, "Four-spherical-mirror zoom telescope continuously satisfying the aplanatic condition," *Opt. Eng.* 28(9), 1014-1018 (1989).
 9. S. Rosin, "Inverse Cassegrainian systems," *Appl. Opt.* 7(8), 1483-1497 (1968).
 10. C. G. Wynne, "Two-mirror anastigmats," *J. Opt. Soc. Am.* 59(5), 572-579 (1969).
 11. B. J. Lin, "The path to subhalf-micrometer optical lithography," in *Optical / Laser Microlithography*, B. J. Lin, ed., Proc. SPIE 922, 256-269 (1988).
 12. R. Hirose, "New g-line lens for next generation," in *Optical / Laser Microlithography II*, B. J. Lin, ed., Proc. SPIE 1088, 178-186 (1989).
 13. W. T. Welford, *Aberrations of the Optical Systems*, pp. 130-152, Adam Hilger Ltd., Bristol (1986).
 14. M. Herzberger, *Modern Geometrical Optics*, pp. 457-462, Interscience, New York (1958).
 15. M. Herzberger, "Gaussian optics and Gaussian brackets," *J. Opt. Soc. Am.* 33, 651-655 (1943).
 16. M. Herzberger, "Precalculation of optical systems," *J. Opt. Soc. Am.* 42, 637-640 (1952).
 17. K. Tanaka, "Paraxial theory in optical design in terms of Gaussian brackets," in *Progress in Optics XXIII*, E. Wolf, ed., pp. 63-111, North-Holland, Amsterdam (1986).
 18. R. W. Daniels, *An Introduction to Numerical Methods and Optimization Techniques*, chap. 8, North-Holland, New York (1978).
 19. D. A. Markle, "The future and potential of optical scanning systems," *Solid State Technol.* 27(9), 159-166 (1984).
 20. 박성찬, UV Submicron Lithography를 위한 4 반사 광학계의 설계 및 수차해석, 한국과학기술원 박사학위 청구논문, 서울 (1991).